Emerging Trends in Engineering and Sustainability (ETES) Volume 01 (No. 01), 2025, pp. 31-36

Emerging Trends in Engineering and Sustainability (ETES)

https://etes.alnaji-uni.edu.iq

https://doi.org/10.65505/ETES-25-0010

ISSN 3105-1723 (Print)
ISSN 3105-1731 (Online)

Al_2O_3 Nano and Micro Films Deposited using PLD on Stainless Steel Substrates for Medical Applications

Hussain Joma Abbas Al Bayaty[1*], Dalya A. Mohammed[2], Abdulhadi Kadhim[2], Noor H. Jumaah[3], Satiye Korkmaz[3], Osman Çiçek[4]

[1] College of engineering, Al-Naji University, Baghdad, Iraq.
[2] College of Laser and Optoelectronic Engineering, University of Technology-Iraq, Baghdad, Iraq.
[3] Department of Electrical and Electronics Engineering, Photonics and Optoelectronics, Faculty of Engineering, Karabuk University, Karabuk, Türkiye.
[4] Department of Electrical and Electronics Engineering, Faculty of Engineering and Architecture, Kastamonu University, Türkiye.

Article Info

Received: 08 November 2025
Revised: 25 December 2025
Accepted: 26 December 2025
Available online:
31 Dec. 2025

Keywords:

304 Stainless Steel;
Al_2O_3;
Corrosion Rate;
PLD

ABSTRACT

In this study, we deposited the Al_2O_3 nanostructure on 304 stainless steel using PLD technique. The stainless-steel specimens were successfully coated with Al_2O_3 nanostructure, and surface morphology was examined using an optical microscope. The findings confirmed the nanostructured nature of the films. Tafel curve analysis was used to determine the polarization of the sample before being subjected to laser shock peening treatment. Additional tests were then carried out on the samples following pulse laser deposition.

1. Introduction

Research has shown that coatings, thin films, and modern alloys applied to the metal surfaces can be used to reduce corrosion. However, to improve the properties of metals—like hardness, roughness, and corrosion resistance—recent studies have used the laser surface treatment of metal for this purpose [1, 2]. A novel technique for treating surfaces is known as "laser shock peening", which has been described as the introduction of mechanical residual stresses as deep compressive shock waves to the surface of the target [3-5]. Concerning this, the obvious option for medical device requirements is the focus on properties of 304 stainless steel. This is because it offers distinctive material features at a competitive price range. Additional important aspects that contribute to the suitability of stainless steel 304 for use in medical purposes include its excellent dependability, manufacturing accuracy, outstanding formability, corrosion resistance, and low carbon content. Additionally, it has been widely used in medical implants and artificial hips, due to its sanitary and simple-to-clean attributes. It has also been utilized in medical equipment such as orthopedic beds, cabinets, and examination machines. For pill hoppers and funnels as well as for piping creams and liquids, pharmaceutical industries have used stainless [6].

For developed surface applications, the coatings have been made using PLD procedures from nanosized grains and metals, which are considered to be some of the promising filters [7, 8]. Due to their exceptional qualities, which are uncommon in conventional coatings, such coatings have considerable promise for a variety of applications. These include heightened

toughness, reduced porosity, elevated corrosion resistance, and wear resistance [9]. The PLD is a process that uses a high-power pulsed laser that is focused in a vacuum chambers to strike the target in order to deposit specific material (thin film) onto a substrate. Furthermore, the PLD method provides a metallurgical bond that is stronger than the mechanical connections produced by plating procedures or spray welding. It also provides regulated and low heat input with little dilution and Heat-Affected Zone (HAZ). Minimal stress and distortion created by the rapid rate of cooling are effective in terms of the cost of manufacturing [10]. Hence, in this study, we used PLD to deposit Al_2O_3 thin films on 304 stainless steel substrates for enhancing the corrosion rate, that is common in various medical applications.

2. Experimental Work

A disk measuring 2 cm in diameter and 6 mm thick was employed. The Al_2O_3 nanomaterial powders used for this were provided by Gamma and were of a high purity (99.95%), with an average particle size of 15 nm. Further, the 304 stainless steel substrates were used for depositing thin films by pulse laser deposition with diameter (20 mm) and thickness of (5 mm). The chemical composition of these samples was determined by using SPECTRO MAXx Instruments (AMETEK materials analysis) located at the "Ministry of Planning Central Organization for Standardization and Quality Control."

All samples were mounted using "EPOXY material (A:B)", which was created by mixing two components by 1:0.5. Then, the sample was placed in a metal mold. This was followed by the addition of the material. After that, time was given for the sample to harden. This was carried out for a quarter-hour before punching a hole through the sample to connect an external wire that touches it from the inside. Through these steps, access was ensured and confirmed. Before starting the erosion process, the sample was placed in the corrosion cells. The avometer device was used to examine the connection between the sample and the wire. It is important to note that the top surface of the sample was left unprotected by this procedure.

2.1 Experimental Set Up of Pulse Laser Deposition (PLD)

The NdYAG laser, target, deposition chamber, substrate heater, substrate, and vacuum system are the core elements of the PLD-system. This procedure was carried out under some essential circumstances, which are listed in Table 1 below.

Table 1. Nano Film parameters of the deposition.

Deposition Parameters	Units	
NanoMaterial	Target	Al_2O_3 nanomaterial
	Substrate	304 stainless steel
Parameter of pulsed Laser	Wavelength, Energy, Repetition rate, Pulse number, Pulse width	700mJ, 532 nm, 150 shot, 3 Hz, 10ns
Pressure parameter	Base pressures	10^{-2} Torr
Target Parameter	Thickness, Diameter	20 mm, 5 mm
Substrate parameter	Temperature, Thickness, Area	0.5cm, 3.14cm², 150C
Distance between	contact "L"	12cm

The PLD procedure was achieved with some steps. First, the pulsed laser deposition experiment was conducted in vacuum chambers, typically at a vacuum level of (10^{-3} Torr). Second, a focused Nd:YAG SHG Q-switching laser beam was used to make a 45° angle with the target surface. Third, the films were applied to substrates made of 304 stainless steel at a temperature of 150 °C and a laser energy of 700 mJ. A Q-switched Nd:YAG laser with SHG operating at 532 nm with a pulse repetition rate of 3 Hz, for 150 shots, was used for the deposition. Before the deposition of the thin film, both the required sample and substrate were ready. It is essential to mention that all procedures of PLD were performed at the "Postgraduate Laboratory/Laser and Optoelectronics Engineering Department, University of Technology."

Some measurement techniques, including XRD, SEM, and AFM, were used to examine the characterizations of the sample in order to test the shape and structure of the Al_2O_3 thin film. This method provided data on phase contrast

measurements, crystal size, crystallization levels, and material composition. In the Shimadzu 6000-XRD, continuous scanning was the selected mode, with a scan velocity of (10 degrees per minute) and an X-ray tube of Cu 1.5406 in the XRD apparatus. The AFM is one of the first apparatus for imaging, scaling, and impacting matter at the nano-scale. AFM, kind Angstrom, Scanning Probe Microscope, development Inc., (SPM-AA-2000), product of USA, were utilized. The microstructure and the ultimate structures of the films were examined using scanning electron microscopy. Additionally, a Filmetrics F20 optical reflectometer was used to measure the thickness of the prepared samples.

3. Results And Discussion

3.1 Results of Chemical Composition

The chemical makeup of the stainless-steel samples was determined by analysis. The element compositions for the samples are listed in Table 2.

Table 2. The Chemical composition of the prepared samples.

Sample	Content
Fe%	Bal.
C%	0.065
Si%	0.262
S%	0.42
Ni%	8.71
P%	0.0269
Mo%	0.588
Cr%	17.93
Al%	0.0046
Mn%	1.48
Cu%	0.436

3.2 Surface Analysis Results

Three types of tests were used for surface analysis for all samples before and after laser treatment, pulse laser deposition and corrosion test, as follows:

3.3 Microstructure Results

The sheet was cut into circular forms with a diameter of 14 mm and a thickness of 2 mm. Next, the circular forms were polished and ground to achieve the same level of surface roughness for all samples. Figure 1 displays the optical microscope picture of one of these samples, following the completion of the laser shock peening surface preparation procedure. Figure 1 also shows the microstructure of the metal's surface, following laser shock peening.

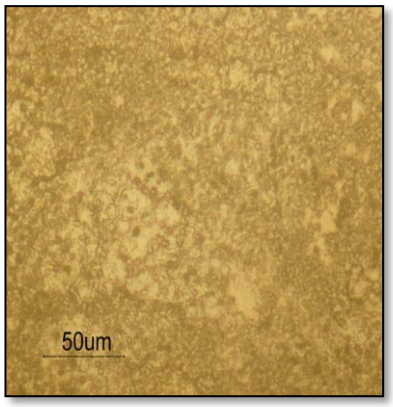

Figure 1. The microstructures of metal's surface with magnification 100X after laser treatment.

3.4 XRD Results

XRD was utilized to quantify the residual stress caused by hardness in heat treated materials [11]. Figure 2 shows the XRD patterns of alloys, which are (A) 304 stainless steel/Al_2O_3 after PLD without LSP and (B) 304 standard stainless steel. The samples were tested under optimum conditions of laser parameters (532 nm, 700 mJ, 4mm and 150 pulses at room temperature). The diffraction peak positions (2θ) of 304 samples/Al_2O_3 after PLD without LSP exhibited at (34.2000^0, 43.3279º, 50.34127º, and 74.4143º) which correspond to (104, 111 and 113, 200, and 220) planes. These are matched with reference [12]. Furthermore, the diffraction peak positions (2θ) of 304 stainless steel /Al_2O_3 alloy with LSP exhibited at (43.3822º and 50.7023º) which correspond to (113 and 024) planes. These are also matched with reference [12, 13]. Finally, the diffraction peak positions (2θ) of standard sample exhibited at (43.3033 º, 50.3897º, and $74.4430^{0)}$ which correspond to (111, 200, and 220) planes. According to reference [14, 15], these are consistent with the standard values of crystal planes. The compressive residual stress at the material surface increased, leading to a higher dislocation density produced by laser shock peening effects [16, 17].

3.5 AFM Results

After PLD, Figure 3 illustrates the results of AFM analysis of the surface layers. It is clearly seen that the surface layer of the samples before and after PLD have much reduced average original grain sizes. However, the average grain size increased to 169.31 nm after PLD. The dislocation movement and dispersion strengthening induced by the LSP process and PLD method were found to be responsible for the refinement of the grain size in the near-surface region. After LSP, an interaction between the laser shock wave and the metal target occurred near the target surface. This subsequently increased the dislocation density and deformed the microstructure close to the surface. Furthermore, the surface roughness decreased to 9.19 nm due to the ablation processes, which are associated with laser shock wave treatment at the surface. [18, 19]

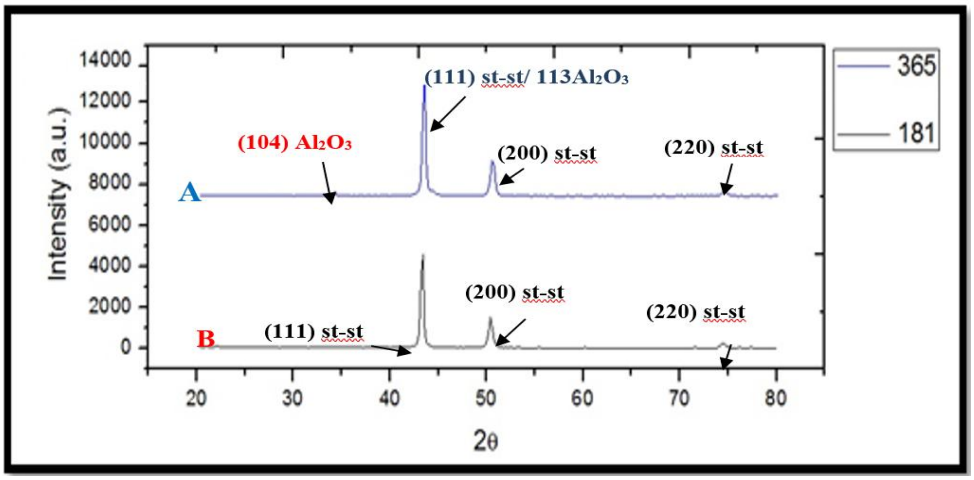

Figure 2. X-RD of patterns (A) 304 stainless steel /Al_2O_3 after PLD without LSP (B) standard samples.

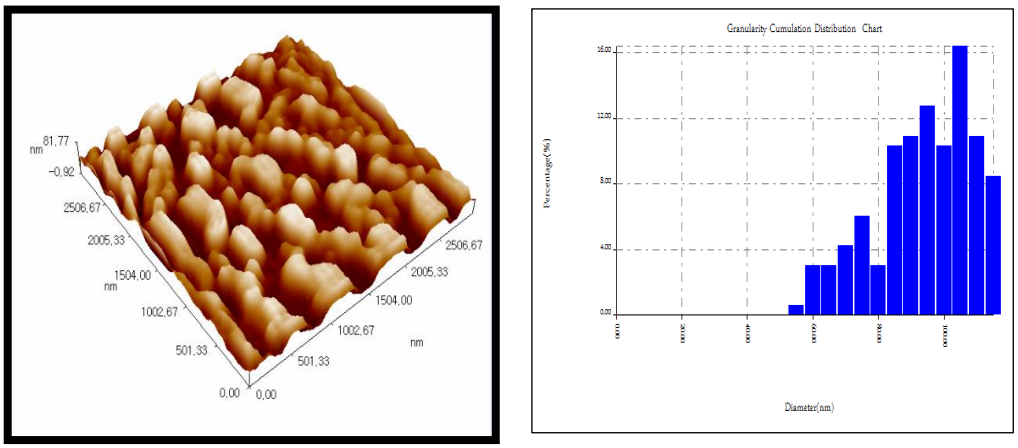

Figure 3. AFM image and histogram of 304 stainless steel /Al_2O_3 after PLD without LSP

Figure 4 illustrates the thickness of the nanofilm deposited using a photo-reflection device. It can be observed that when the pulse count increased from 50 to 150 pulses, an increase in the Nano film thickness was noticed. This increase indicates a strong correlation with positive changes in grain size, resulting in the sustainment of smoother surface. After 200 pulses, the thickness decreased from 415 nm to 295 nm as the pulse count increased from 150 to 250 pulses [20, 21].

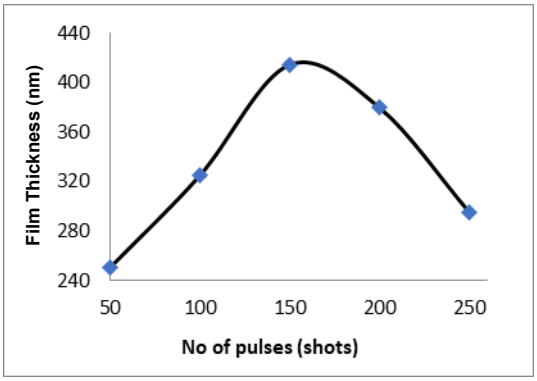

Figure 4. Film thickness versus Number of pulses of Al_2O_3 nanostructures

4. Conclusions

The Al_2O_3 nano-structure results show that the coating is free of cracks, uniform, and compact. It was deposited on 304 stainless-steel using the PL technique, with and without the addition of PEG. The morphological observations (optical microscopy) and measurements of the Al_2O_3-coated stainless-steel specimens confirm the nano-structured nature of the films.

Acknowledgements

The authors thank the lab teams at Al-Naji University and University of Technology-Baghdad for their assist in conducting the results of the current research.

Conflict of interest

The authors declare no conflicts of interest concerning this research.

Funding

No funding was received for conducting this study.

Author Contribution

H. JA. Al Bayaty, N.H. Jumaah, and **D.A. Mohammed** proposed the research problem.

A. Kadhim and **N.H. Jumaah** developed the theoretical framework.

S. Korkmaz, H. JA. Al Bayaty, and **O. Çiçek** verified the analytical methods.

All authors participated in the discussion of the results and contributed to writing the manuscript.

AI Declaration Statement

The authors confirm that the manuscript has been written without the assistance of generative AI or AI-based writing tools.

References

[1] D. A. Mohammed, M. A. Fakhri, and A. Kadhim, "Reduction the Corrosion Rate of 304 Stainless Steel using Pulsed Laser Shock Penning Method," *IOP Conference Series: Materials Science and Engineering,* vol. 454, no. 1, p. 012162, 2018/12/01 2018, doi: 10.1088/1757-899X/454/1/012162.

[2] J. Grum, "Comparison of different techniques of laser surface hardening," *Journal of Achievements in Materials and Manufacturing Engineering,* vol. 24, no. 1, pp. 17-25, 2007.

[3] Y. Xiong, T. He, Z. Guo, H. He, F. Ren, and A. A. Volinsky, "Effects of laser shock processing on surface microstructure and mechanical properties of ultrafine-grained high carbon steel," *Materials Science and Engineering: A,* vol. 570, no. May, pp. 82-86, 2013/05/15/ 2013, doi: https://doi.org/10.1016/j.msea.2013.01.068.

[4] M. A. Fakhri, S. F. H. Alhasan, N. H. Numan, J. M. Taha, and F. G. Khalid, "Effects of laser wavelength on some of physical properties of Al_2O_3 nano films for optoelectronic device," *AIP Conference Proceedings,* vol. 2213, no. 1, p. 020227, 2020, doi: https://doi.org/10.1063/5.0000183.

[5] S. S. Kubsad, B. Siddeswarappa, and B. Sridhar, "Effect of shock waves on wear behavior of few metallic materials," *International Journal of Engineering Science and Technology (IJEST),* vol. 4, no. 5, pp. 2425-2431, 2012.

[6] A. A. Al-Amiery, F. A. Binti Kassim, A. A. H. Kadhum, and A. B. Mohamad, "Synthesis and characterization of a novel eco-friendly corrosion inhibition for mild steel in 1 M hydrochloric acid," *Scientific Reports,* vol. 6, no. 1, p. 19890, 2016/01/22 2016, doi: https://doi.org/10.1038/srep19890.

[7] I. A. Abbas and K. H. Al-Mayalee, "Structural and Optical Properties of Al_2O_3 Nanostructures Prepared by Hot Water Treatment Method," *Revue des Composites et des Materiaux Avances,* vol. 34, no. 4, pp. 527-532, 2024, doi: https://doi.org/10.18280/rcma.340414.

[8] M. H. Ayman *et al.*, "Hardness Optimization Using Takeuchi and ANOVA Method for Al_2O_3 Nano-Coating by PLD Systems," *International Journal of Nanoelectronics and Materials (IJNeaM),* vol. 18, no. June,

pp. 269-279, 07/23 2025, doi: https://doi.org/10.58915/ijneam.v18iJune.2363.

[9] G. E. Stan *et al.*, "Critical advances in the field of magnetron sputtered bioactive glass thin-films: An analytical review," *Applied Surface Science,* vol. 646, no. February, p. 158760, 2024/02/15/ 2024, doi: https://doi.org/10.1016/j.apsusc.2023.158760.

[10] K. Shahapurkar *et al.*, "Comprehensive review on polymer composites as electromagnetic interference shielding materials," *Polymers and Polymer Composites,* vol. 30, no. 1, p. 09673911221102127, 2022, doi: https://doi.org/10.1177/09673911221102127.

[11] V. F. Nunes, P. H. F. Maia, A. F. L. Almeida, and F. N. A. Freire, "Surface properties of Al2O3:ZnO thin films growth on FTO for photovoltaic application," *Next Materials,* vol. 2, no. January, p. 100069, 2024/01/01/ 2024, doi: https://doi.org/10.1016/j.nxmate.2023.100069.

[12] J. M. Taha, R. A. Nassif, N. H. Numan, and M. A. Fakhri, "Effects of oxygen gas on the physical properties of tin oxide nano films using laser light as ablation source," *AIP Conference Proceedings,* vol. 2213, no. 1, p. 020235, 2020, doi: https://doi.org/10.1063/5.0000198.

[13] M. I. Ahmed, H. S. Jahin, H. A. Dessouki, and M. Y. Nassar, "Synthesis and characterization of γ-Al_2O_3 and α-Al2O3 nanoparticles using a facile, inexpensive auto-combustion approach," *Egyptian Journal of Chemistry,* vol. 64, no. 5, pp. 2509-2515, 2021, doi: https://doi.org/10.21608/ejchem.2021.61793.3330.

[14] P. S. Prevéy, "The measurement of subsurface residual stress and cold work distributions in nickel base alloys," in *ASM's conference on residual stress in design, process and materials selection*, Cincinnati, Ohio, USA, W. B. Young, Ed., 1987: ASM International, pp. 11-20.

[15] R. A. Abeer, A. A. Ali, A. F. Makram, A. Q. Motahher, and C. B. G. Subash, "Optical properties of Al_2O_3 thin film deposited by pulsed laser deposition technique," *International Journal of Nanoelectronics and Materials (IJNeaM),* vol. 18, no. 2, pp. 256-262, 05/05 2025, doi: https://doi.org/10.58915/ijneam.v18i2.2124.

[16] H.-J. Kim and S.-M. Nam, "High loading of nanostructured ceramics in polymer composite thick films by aerosol deposition," *Nanoscale Research Letters,* vol. 7, no. 1, p. 92, 2012/01/27 2012, doi: https://doi.org/10.1186/1556-276X-7-92.

[17] S. Y. Lee, E. W. Huang, W. Woo, C. Yoon, H. Chae, and S.-G. Yoon, "Dynamic Strain Evolution around a Crack Tip under Steady- and Overloaded-Fatigue Conditions," *Metals*, vol. 5, no. 4, pp. 2109-2118doi: https://doi.org/10.3390/met5042109.

[18] M. A. Fakhri *et al.*, "Effect of different laser wavelengths on the optical properties of GaN/PSi and Al_2O_3/PSi thin films using the pulse laser deposition method," *Journal of Optics,* vol. 53, no. 5, p. 02393, 2024/12/30 2024, doi: https://doi.org/10.1007/s12596-024-02393-w.

[19] N. E. Naji, A. A. Aljubouri, and R. A. Ismail, "Structural Characteristics of Alumina Nanoparticles Synthesised by DC Reactive Sputtering Technique," *Journal of Applied Sciences and Nanotechnology,* vol. 5, no. 3, pp. 13-23, 2025, doi: https://doi.org/10.53293/jasn.2025.7575.1335.

[20] E. Sivasenthil, R. Nandhini, D. Tamilselvi, and R. Raja, "Synthesis and characterization of Al2O3 nanoparticles by using co-precipitation method," *AIP Conference Proceedings,* vol. 2861, no. 1, p. 020008, 2023, doi: https://doi.org/10.1063/5.0160270.

[21] D. A. Mohammed, A. Kadhim, and M. A. Fakhri, "The enhancement of the corrosion protection of 304 stainless steel using Al2O3 films by PLD method," *AIP Conference Proceedings,* vol. 2045, no. 1, p. 020014, 2018, doi: https://doi.org/10.1063/1.5080827.